

[3]FERROCENOPHANE BRIDGE REVERSAL BARRIERS

I. SULPHUR, SELENIUM AND TELLURIUM BRIDGING ATOMS

EDWARD W. ABEL, MARTIN BOOTH and KEITH G. ORRELL

Department of Chemistry, The University, Exeter EX4 4QD (Great Britain)

(Received September 5th, 1980)

Summary

Dynamic NMR studies have yielded accurate energy data for the bridge reversal fluxion of [3]ferrocenophanes with Group VI bridging atoms. This process, whilst appearing very analogous to the chair-to-chair reversal of corresponding 6-membered heterocyclic rings, appears to be a much higher energy process, its associated ΔG^\ddagger values being in the range 59 to 81 kJ mol⁻¹ depending on the types of Group VI bridging atoms. These data allow estimates to be made for the first time of the relative magnitudes of torsional barriers about single bonds involving like and unlike Group VI atoms. For example, the S–S torsion is shown to be 3.9 kJ mol⁻¹ higher in energy than the S–Se torsion and 5.8 kJ mol⁻¹ higher than the Se–Se torsion. The probable mechanism of the bridge reversal process is discussed.

Introduction

We have recently applied accurate dynamic NMR band shape fitting methods to the determination of energy barriers associated with a variety of fluxional phenomena [1–3]. Of particular interest have been the barriers to six-membered ring reversal in compounds containing Group VI atoms [1,3]. As an extension to these studies we have recently shown that the bridge reversal fluxion observed for [3]ferrocenophanes [4–7] is analogous to six-membered ring reversal [8,9] and have determined the energy of bridge reversal for 1,2,3-trithia[3]ferrocenophane [10]. We have now accurately calculated the bridge reversal barriers for a large number of [3]ferrocenophanes, and report here our results for the trichalcogen series $[(\eta\text{-C}_5\text{H}_4)_2\text{FeX}_2\text{Y}]$ (X = S or Se; Y = S, Se or Te) ($\equiv \text{Cp}_2\text{FeX}_2\text{Y}$ in the text hereon) [11].

TABLE 1
 CHEMICAL SHIFTS AND THEIR TEMPERATURE-VARIABLE COEFFICIENTS FOR THE CYCLOPENTADIENYL HYDROGENS^a

Compound	Solvent	Reference	ν_A (Hz)		ν_B (Hz)		ν_C (Hz)		ν_D (Hz)	
			a	b	a	b	a	b	a	b
Cp ₂ FeS ₃	C ₆ D ₅ NO ₂	HMDS	431.7	0.000	425.0	0.013	417.5	0.013	361.2	0.020
Cp ₂ FeS ₂ Se	C ₆ D ₅ NO ₂	HMDS	430.7	0.000	423.1	0.000	411.2	0.019	357.2	0.019
Cp ₂ FeS ₂ Te	CDCl ₃	TMS	448.6	-0.072	440.5	-0.072	419.3	-0.072	390.0	-0.015
Cp ₂ FeSe ₂ S	C ₆ D ₅ NO ₂	HMDS	431.0	0.000	421.2	0.000	423.8	0.000	367.3	0.000
Cp ₂ FeSe ₃	C ₆ D ₅ CD ₃	HMDS	403.1	0.035	372.4	0.136	370.5	0.136	348.9	0.106
Cp ₂ FeSe ₂ Te	CDCl ₃	TMS	445.0	-0.086	438.1	-0.046	424.3	-0.086	397.2	-0.064

^a Chemical shift (ν_i) from HMDS or TMS (in Hz) at temperature θ_c /°C is given by the expression $\nu_i(\text{Hz}) = a + b(\theta_c/^\circ\text{C})$.

Experimental

The variable temperature 100 MHz ^1H NMR spectra were recorded in a variety of solvents (see Table 1 for details) on a JEOL MH-100 or PS/PFT-100 spectrometer, the FT instrument being used for the less soluble compounds. A JES-VT-3 unit was used to control the probe temperature and the spectra were recorded at 5–10°C intervals over as wide a temperature range as permitted by the solvent. The temperature measurements were made using a thermocouple adapted for use in the NMR probe. These measurements were made before and after recording the spectra and temperatures are considered accurate to at least $\pm 1^\circ\text{C}$.

Results

In order to calculate the bridge reversal energy barrier, values of the rate constant, k , for this fluxional process need to be determined at a series of temperatures. Such data were obtained by accurate DNMR analysis of the

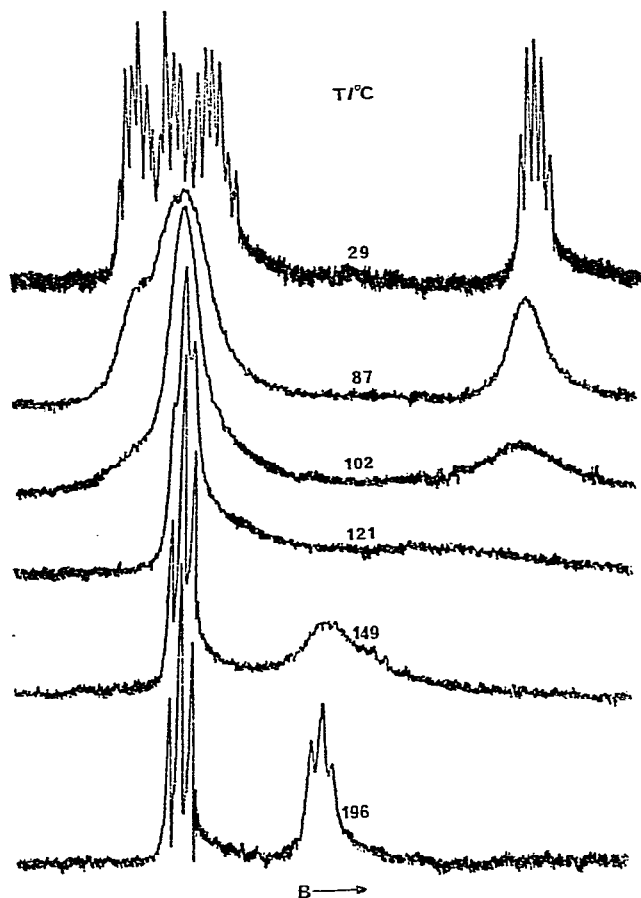


Fig. 1. Variable temperature spectra of $\text{Cp}_2\text{FeS}_2\text{S}$.

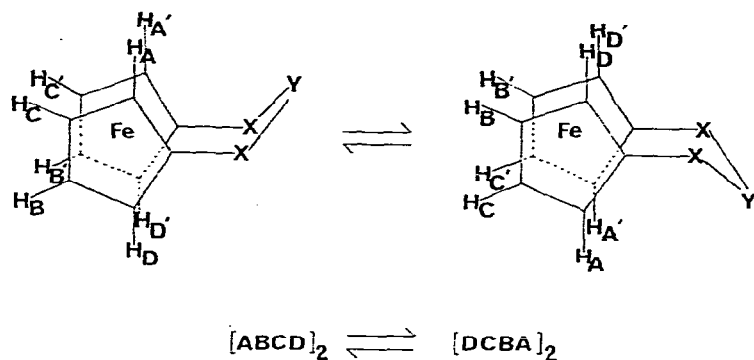


Fig. 2. Static conformations and nuclear spin system for the [3]ferrocenophanes.

variable temperature ^1H spectra, ^1H studies being used in preference to ^{13}C because the more complex proton spectral band shapes are more sensitive to theoretical simulation and therefore provide more accurate k values [12].

All the spectra obtained were of a basically similar nature, as illustrated by those for $\text{Cp}_2\text{FeS}_2\text{S}$, Fig. 1, different bridging chalcogens producing only relatively small variations in internal chemical shifts and consequently band coalescences at different temperatures. The "static" (low temperature) spectra consist of four complex signals which, upon raising the sample temperature, first collapse and then eventually give two distorted triplets at high temperatures. The "static" spectra may be rationalised by considering the static conformation of the [3]ferrocenophanes, Fig. 2. This conformation possesses a reflection plane through the Fe and Y atoms resulting in chemical equivalence of the two cyclopentadienyl (Cp) rings. The four protons in each ring are anisochronous and each proton has an isochronous but magnetically non-equivalent counterpart in the other Cp ring, giving rise to an $[\text{ABCD}]_2$ nuclear spin system. Inspection of the static spectra shows that no long range $^4J(\text{H}-\text{C}-\text{Fe}-\text{C}-\text{H})$ couplings between the protons on different Cp rings could be detected; and hence the spin system can be reduced to ABCD without error. An alternative static conformation consisting of staggered Cp rings [6] will also give rise to the observed ABCD spectra but may be discounted as a result of recent NMR

TABLE 2

SPIN-SPIN COUPLING CONSTANTS (Hz) FOR THE CYCLOPENTADIENYL HYDROGENS, AND THEIR EFFECTIVE TRANSVERSE RELAXATION TIMES (s)^a

Compound	J_{AB}	J_{AC}	J_{AD}	J_{BC}	J_{BD}	J_{CD}	T_2^*
Cp_2FeS_3	1.25	2.53	1.23	2.44	2.52	1.24	0.400
$\text{Cp}_2\text{FeS}_2\text{Se}$	1.31	2.49	1.22	2.49	2.54	1.25	0.318
$\text{Cp}_2\text{FeS}_2\text{Te}$	1.33	2.49	1.28	2.52	2.52	1.30	0.318
$\text{Cp}_2\text{FeSe}_2\text{S}$	1.25	2.50	1.25	2.50	2.50	1.25	0.400
Cp_2FeSe_3	1.26	2.53	1.23	2.44	2.52	1.24	0.400
$\text{Cp}_2\text{FeSe}_2\text{Te}$	1.25	2.46	1.25	2.39	2.43	1.26	0.256

^a T_2^* determined from $\Delta\nu_{1/2} = (\pi T_2^*)^{-1}$, where $\Delta\nu_{1/2}$ = natural line width at half-height.

[7] and crystallographic evidence [13]. The onset of rapid bridge reversal will average the protons as shown in Fig. 2 and illustrated by the spectra of Fig. 1.

The spectral parameters required for DNMR analysis were extracted from the static spectra by simulation using the LAOCNR computer program, Fig. 3. The data obtained for all six complexes are illustrated in Tables 1 and 2.

The chemical shift data include temperature variations measured over at least a 30°C range. Accurate analysis of the spectra in this way led to the unambiguous assignment of protons A and D of Fig. 2 to the highest and lowest frequency signals, 4 and 1 of Fig. 3, in all cases. Proton D was tentatively assigned to the lowest frequency signal 1 on the assumption that it experienced the greater shielding due to the axial lone pair of X. It should be noted, however, that the correct assignment of protons A and D is not essential for DNMR analysis. However, once the assignments of proton D to signal 1 and proton A to signal 4 have been made it becomes crucial to assign protons B and C correctly since a reversal of their assignments significantly changes the computer simulated spectrum. Our results showed that in all but one of the compounds the experimental spectra could only be satisfactorily simulated by assigning proton B to signal 3 and proton C to signal 2. The exception was $\text{Cp}_2\text{FeSe}_2\text{S}$ where the assignments of protons B and C needed to be reversed. This assignment of proton B to signal 3 is surprising since from simple shielding arguments one would expect proton C, being adjacent to A, to be responsible for the second highest frequency signal, whereas this is the case only for $\text{Cp}_2\text{FeSe}_2\text{S}$.

Having successfully obtained the "static" NMR parameters it was possible to simulate the exchanging spectra as an $\text{ABCD} \rightleftharpoons \text{DCBA}$ spin problem using the DNMR 36 computer program [2]. In this way bridge reversal rate constants were obtained for a series of temperatures often covering a range of over 100°C.

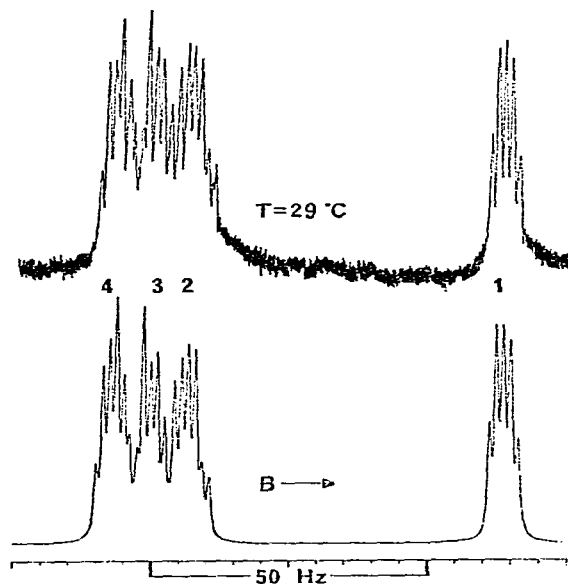


Fig. 3. Static spectrum of $\text{Cp}_2\text{FeS}_2\text{S}$ and its computer simulation.

TABLE 3
ARRHENIUS AND ACTIVATION PARAMETERS FOR [3]FERROCENOPHANE BRIDGE REVERSAL

Compound	Solvent	$T_c(AD)$ (K)	$T_c(BC)$ (K)	E_a (kJ mol ⁻¹)	$\log_{10} A$	ΔH^\ddagger (kJ mol ⁻¹)	ΔS^\ddagger (J K ⁻¹ mol ⁻¹)	$\Delta G^\ddagger a$ (kJ mol ⁻¹)
Cp ₂ FeS ₃	C ₆ D ₅ NO ₂	401	353	80.3 ± 0.9	12.7 ± 0.1	77.0 ± 0.9	-11.7 ± 2.3	80.4 ± 0.2
Cp ₂ FeS ₂ Se	C ₆ D ₅ NO ₂	354	332	72.9 ± 1.1	12.8 ± 0.2	69.8 ± 1.1	-9.5 ± 2.9	72.6 ± 0.2
Cp ₂ FeS ₂ Te	CDCl ₃	309	285	63.0 ± 1.3	12.9 ± 0.2	60.5 ± 1.3	-6.8 ± 4.3	62.5 ± 0.02
Cp ₂ FeSe ₂ S	C ₆ D ₅ NO ₂	352	303	70.2 ± 0.9	12.6 ± 0.1	67.3 ± 0.8	-12.4 ± 2.4	71.0 ± 0.1
Cp ₂ FeSe ₃	C ₆ D ₅ CD ₃	323	287	68.4 ± 2.4	13.0 ± 0.4	65.8 ± 2.4	-5.0 ± 7.8	67.2 ± 0.1
Cp ₂ FeSe ₂ Te	CDCl ₃	289	280	59.4 ± 1.1	12.7 ± 0.2	57.0 ± 1.1	-9.8 ± 3.5	59.9 ± 0.1

^a Calculated for T = 298.15 K.

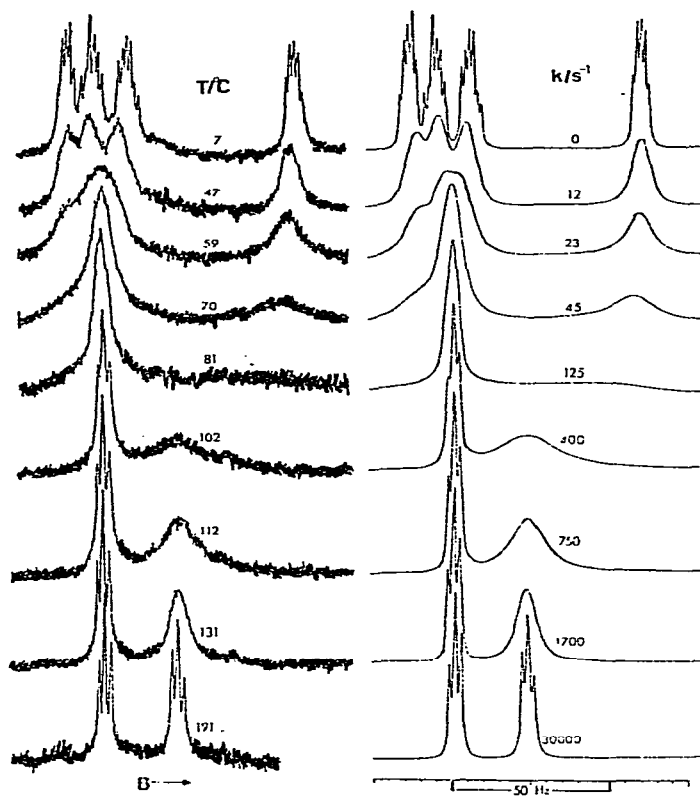


Fig. 4. Examples of band shape fittings for $\text{Cp}_2\text{FeS}_2\text{Se}$.

Examples of the band shape fittings for $\text{Cp}_2\text{FeS}_2\text{Se}$ are illustrated in Fig. 4. Simulation of the ^1H NMR spectra have led to what are considered to be very accurate values of the exchange rate constants due to the complexity of the experimental spectra both above and below coalescence and to the gross changes in line shape over the wide temperature range studied.

The data so obtained were utilised to give the Arrhenius and activation parameters listed in Table 3. The errors quoted for ΔH^\ddagger and ΔS^\ddagger are standard deviations (σ) based on least squares fittings of the experimental data using the THERMO computer program [14]. Following the treatment of Binsch et al. [15] the errors quoted for ΔG^\ddagger are given by $\sigma(\Delta G^\ddagger) = |\sigma(\Delta H^\ddagger) - T\sigma(\Delta S^\ddagger)|$. This treatment explains why ΔG^\ddagger is the activation parameter least prone to statistical error and why energy barriers of rate processes are usually most meaningfully discussed in terms of this parameter.

Discussion

The chemical shift data in Table 1 reveal a number of interesting features, although care must be taken in their interpretation in view of the variety of solvents and reference materials used. Our discussion is therefore confined to internal chemical shifts, Table 4. The values of $\nu_A - \nu_D$ and $\nu_B - \nu_C$ decrease

TABLE 4

INTERNAL CHEMICAL SHIFTS (Hz) FOR THE [3]FERROCENOPHANE CYCLOPENTADIENYL PROTONS

Compound	Cp ₂ FeS ₃	Cp ₂ FeS ₂ Se	Cp ₂ FeS ₂ Te	Cp ₂ FeSe ₂ S	Cp ₂ FeSe ₃	Cp ₂ FeSe ₂ Te
$\nu_A - \nu_D$	70.5	73.5	58.6	63.7	54.4	47.8
$\nu_B - \nu_C$	7.5	11.9	21.2	-2.6	1.9	13.8

as the size of the heteroatoms adjacent to the Cp rings increases, i.e. S₂Y > Se₂Y, (Y = S, Se or Te). This result presumably reflects a reduction in the shielding of the Cp protons as the C—X bond length increases. Similarly, increasing the size of the central bridging atom Y brings about a decrease in $\nu_A - \nu_D$, whilst in contrast $\nu_B - \nu_C$ increases, as shown by the species Se₂S, Se₂Se and Se₂Te. It is difficult to rationalize these latter changes but they almost certainly reflect a change in the angular relationship between the X₂Y bridge and the two Cp rings as a result of the change in size and electronic nature of Y. The coupling constants listed in Table 2 show little or no variation from those determined previously for bridged ferrocene compounds [16], confirming the invariant geometry of the individual Cp rings.

The values for the Gibbs free energy of activation, ΔG^\ddagger , for bridge reversal listed in Table 3 show a number of trends which relate to the bridge reversal mechanism. In particular they confirm our previous postulate that the bridge reversal process is analogical to six-membered ring reversal [10] (see below).

TABLE 5

THE DEPENDENCE OF BRIDGE REVERSAL BARRIERS UPON THE BRIDGE LENGTH (C—X—Y—X—C)

Bridging atoms	Bridge length (pm)	ΔG^\ddagger (kJ mol ⁻¹)
	778	80.4
	804	72.6
	830	71.0
	856	67.2
	844	62.5
	896	59.9

The values of ΔG^\ddagger exhibit a marked correlation with the total length of the [3]ferrocenophane bridge (C—X—Y—X—C) determined from covalent radii, Table 5. The only values out of sequence are those for the Se_2Se and S_2Te species. Such a dependence is also observed for six-membered ring reversal where large bond lengths generally lead to lower ring reversal barriers [8,9,17]. In the case of six-membered ring reversal it is more informative to relate the changes to variations in torsional barriers about the bonds which constitute the ring [17]. The same is also true for the [3]ferrocenophanes and this explains the discrepancy for the Se_2Se and S_2Te species mentioned above, where, although the S—Te bond length (241 pm) is not much greater than that for Se—Se (234 pm), the torsional barrier and, therefore, ΔG^\ddagger are considerably less. In the case of the [3]ferrocenophanes we can determine a rough estimate of the relative C—X and X—Y torsional barriers provided that the contribution to ΔG^\ddagger from the Cp_2Fe part of the molecule is constant throughout the series. Consider the bridge reversal energies obtained for $\text{Cp}_2\text{FeS}_2\text{Se}$ (72.6 kJ mol^{-1}) and $\text{Cp}_2\text{FeSe}_2\text{S}$ (71.0 kJ mol^{-1}). The only differences between the two molecules in terms of torsional vibrations are two C—Se bonds instead of two C—S bonds. Thus, assuming all other contributions to the overall energy barrier remain constant, the difference between the C—S and C—Se torsional barriers $\{\Delta\Delta G^\ddagger(\text{C—X})\}$ is given by $(72.6 - 71.0)/2 = 0.8 \text{ kJ mol}^{-1}$. This value can be compared with the value of 2.4 kJ mol^{-1} found for the difference between Me—S and Me—Se torsional barriers in Me—X—Me compounds [17]. Although the difference between those two values is small it may well reflect the different electronic environments of the carbon atoms in these two types of C—X bonds. With the aid of the above data it is possible

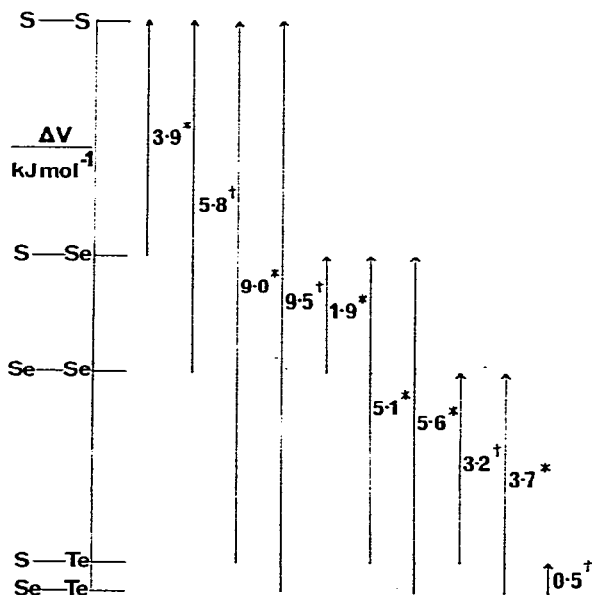


Fig. 5. Relative torsional barriers (ΔV) determined from bridge reversal barriers. * Calculated from $\{\Delta G^\ddagger(1) - \Delta G^\ddagger(2)\}/2$; † Calculated from $\{\Delta G^\ddagger(1) - \Delta G^\ddagger(2)\}/2 \pm \Delta\Delta G^\ddagger(\text{C—X})$.

to calculate a variety of other relative torsional barriers and these are illustrated in Fig. 5. For example, the relative torsional barriers about S—S compared to Se—Se bonds may be calculated from the values of ΔG^\ddagger for $\text{Cp}_2\text{FeS}_2\text{S}$ ($\Delta G^\ddagger(1) = 80.4 \text{ kJ mol}^{-1}$) and $\text{Cp}_2\text{FeSe}_2\text{Se}$ ($\Delta G^\ddagger(2) = 67.2 \text{ kJ mol}^{-1}$). This energy difference of 13.2 kJ mol^{-1} is accounted for by considering the different torsional vibrations of the two molecules i.e. $2(\text{C—S}) + 2(\text{S—S})$ vibrations compared with $2(\text{C—Se}) + 2(\text{Se—Se})$ vibrations. Now assuming C—S torsional barriers are 0.8 kJ mol^{-1} greater than C—Se torsional barriers, then the difference between S—S and Se—Se torsional barriers is given by $\{13.2 - (2 \times 0.8)\} / 2 = 5.8 \text{ kJ mol}^{-1}$. The values given in Fig. 5 show the relative torsional barriers (ΔV) about single bonds involving like and unlike Group VI atoms, such data having previously been unobtainable because of the difficulties in synthesising suitable compounds.

Other authors [18,19] have postulated a decrease in torsional barriers for R—X—X—R species ($X = \text{S, Se or Te}$) as the size of the heteroatoms increase. However, to our knowledge no experiments have been performed to determine torsional barriers for compounds with $X = \text{Se or Te}$. In the case of $X = \text{S}$ a variety of physical methods have been applied [20] and the most reliable values of S—S torsional barriers appear to be 29.3 kJ mol^{-1} for dibenzyl disulphide [21] and 28.5 kJ mol^{-1} for dimethyl disulphide [22]. Assuming a value of 29 kJ mol^{-1} for the S—S torsional barrier in [3]ferrocenophanes it is now possible to determine the torsional barriers for bonds between other homonuclear and heteronuclear Group VI atoms using the data in Fig. 5. Thus the Se—Se torsional barrier will equal $(29 - 5.8)$ or 23.2 kJ mol^{-1} . Similarly, the estimated barriers for S—Se, S—Te and Se—Te torsions are 25.1 , 20.0 and 19.5 kJ mol^{-1} , respectively. Our values show the expected decrease in torsional barriers as the bond length increases, reflecting the reduction in lone pair interactions during bond rotation.

We have clearly seen that bridge reversal in [3]ferrocenophanes is closely analogous to six-membered ring reversal both in terms of the static conformations and the influence of torsional barriers upon the bridge reversal barrier. It is now possible to postulate a mechanism for the bridge reversal process. It has already been shown that in going from the one pseudo-chair conformation of [3]ferrocenophane to the other a planar transition state is energetically unfavourable [4]. A much more likely mechanism involves rotation about the Cp—Fe and bridge C—X and X—Y bonds giving a conformation which possesses staggered Cp rings and resembles the half chair conformation of cyclohexane, Fig. 6. It is impossible to say whether this half chair type of conformation is a true high energy intermediate or a transition state species. However, its lack of detection by $^1\text{H NMR}$ indicates that its energy must be considerably higher (and its population correspondingly lower) than the pseudochair conformation.

Finally it is of interest to contrast the energy barrier for bridge reversal with that for the analogous six-membered ring reversal. Of the six compounds studied only $\text{Cp}_2\text{FeS}_2\text{S}$ has a known analogue, $(\text{CH}_2)_3\text{S}_3$, and it is most notable that for this case our bridge reversal barrier is ca. 25 kJ mol^{-1} greater than the corresponding ring reversal barrier [23]. In order to obtain more information about the relative magnitudes of energy barriers for the two processes, we have synthesised a variety of other [3]ferrocenophanes, namely $\text{Cp}_2\text{FeX}_2\text{Y}$ ($X = \text{CH}_2$;

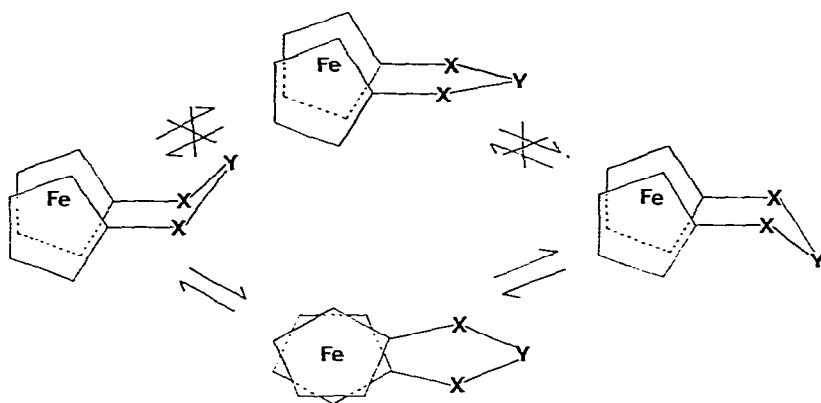


Fig. 6. Mechanisms for [3]ferrocenophane bridge reversal.

Y = CH₂, O or S. X = S, Y = CH₂ or CMe₂), which have appropriate six-membered ring analogues. The results for these compounds are given in the following paper [24].

Acknowledgements

We are indebted to Mr. R.E. Hollands and Dr. A.G. Osborne for their generous donation of samples, and to Dr. V. Šik for recording a number of the ¹H NMR spectra.

References

- 1 E.W. Abel, M. Booth and K.G. Orrell, *J. Organometal. Chem.*, **160** (1978) 75.
- 2 E.W. Abel, M. Booth and K.G. Orrell, *J. Chem. Soc. Dalton*, (1979) 1994.
- 3 E.W. Abel, M. Booth and K.G. Orrell, *J. Chem. Soc. Dalton*, (1980) 1582.
- 4 M. Rosenblum, A.K. Banerjee, N. Danieli, R.W. Fish and V. Schlatter, *J. Amer. Chem. Soc.*, **85** (1963) 316.
- 5 T.H. Barr and W.E. Watts, *Tetrahedron*, **24** (1968) 6111.
- 6 A. Davison and J.C. Smart, *J. Organometal. Chem.*, **19** (1969) P7.
- 7 A. Davison and J.C. Smart, *J. Organometal. Chem.*, **174** (1979) 321.
- 8 I.O. Sutherland, *Ann. Reports NMR Spectroscopy*, **5** (1969) 83.
- 9 F.A.L. Anet and R. Anet in L.M. Jackman and F.A. Cotton (Eds.), *Dynamic Nuclear Magnetic Resonance Spectroscopy*, Academic Press, New York, 1975, p. 543.
- 10 E.W. Abel, M. Booth and K.G. Orrell, *J. Organometal. Chem.*, **186** (1980) C37.
- 11 R.E. Hollands, A.G. Osborne and I. Townsend, *Inorg. Chim. Acta*, **37** (1979) L541.
- 12 G. Binsch in L.M. Jackman and F.A. Cotton (Eds.), *Dynamic Nuclear Magnetic Resonance Spectroscopy*, Academic Press, New York, 1975, p. 45.
- 13 I. Bernal and B.R. Davis, *J. Cryst. Mol. Struct.*, **2** (1972) 107; A.G. Osborne, R.E. Hollands, J.A.K. Howard and R.F. Bryan, *J. Organometal. Chem.*, **205** (1981) 395.
- 14 V. Šik, personal communication.
- 15 D. Hofner, I. Tamir and G. Binsch, *Org. Magn. Reson.*, **11** (1978) 172; G. Binsch and H. Kessler, *Angew. Chem. (Intern. Ed.)*, **19** (1980) 411.
- 16 R.R. McGuire, R.E. Cochoy and J.A. Winstead, *J. Organometal. Chem.*, **84** (1975) 269.
- 17 J.B. Lambert and S.I. Featherman, *Chem. Rev.*, **75** (1975) 611.
- 18 G.C. Pappalardo, J.K. Irgolic and R.A. Grigsby, *J. Organometal. Chem.*, **133** (1977) 311.
- 19 M. Baldo, A. Forchioni, K.J. Irgolic, G.C. Pappalardo, *J. Amer. Chem. Soc.*, **100** (1978) 97.
- 20 N. Allinger, M.J. Hickey and J. Kao, *J. Amer. Chem. Soc.*, **98** (1976) 2741.

- 21 R.R. Fraser, G. Boussard, J.K. Saunders, J.B. Lambert and C.E. Mixan, *J. Amer. Chem. Soc.*, **93** (1971) 3822.
- 22 W.N. Hubbard, D.R. Douslin, J.P. McCullough, D.W. Scott, S.S. Todd, J.F. Messerley, I.A. Hossenlopp, A. George and G. Waddington, *J. Amer. Chem. Soc.*, **80** (1958) 3547.
- 23 S. Kabuss, A. Luttringhaus, H. Friebohn and R. Mecke, *Z. Naturforsch. B*, **21** (1966) 320.
- 24 E.W. Abel, M. Booth, C.A. Brown, K.G. Orrell and R.L. Woodford, *J. Organometal. Chem.*, to be published.